Heliyon

*Received:*
16 April 2018
*Revised:*
13 June 2018
*Accepted:*
27 June 2018

Cite as: Jenifer Trepiana, M. Begoña Ruiz-Larrea, José Ignacio Ruiz-Sanz. Unraveling the *in vitro* antitumor activity of *Vismia baccifera* against HepG2: role of hydrogen peroxide. Heliyon 4 (2018) e00675. doi: 10.1016/j.heliyon.2018.e00675

# Unraveling the *in vitro* antitumor activity of *Vismia baccifera* against HepG2: role of hydrogen peroxide

**Jenifer Trepiana, M. Begoña Ruiz-Larrea*, José Ignacio Ruiz-Sanz**

*Department of Physiology, Medicine and Nursing School, University of the Basque Country UPV/EHU, Leioa 48940, Spain*

* Corresponding author.

E-mail address: mbego.ruizlarrea@ehu.eus (M.B. Ruiz-Larrea).

## Abstract

Currently natural products derived from plants are receiving huge attention because of their antitumor activities. In previous work we reported that an aqueous leaf extract of *Vismia baccifera* induced toxicity in HepG2. The present study focuses on the mechanisms of the cytotoxic actions induced by the extract. Results showed that *V. baccifera* was innocuous in non-transformed human HH4 hepatocytes. In HepG2 it caused deregulation of antioxidant status (increasing superoxide dismutase expression and decreasing glutathione levels and glutathione peroxidase activity) and accumulation of reactive oxygen species, particularly hydrogen peroxide. The extract induced a) cell cycle arrest at $G_2$/M phase, b) phosphorylation of ATM (protein kinase ataxia-telangiectasia mutated) and γH2AX (γ-histone family 2A variant), c) caspase-3 activation, and e) deregulation of the Bax/Bcl family, increasing pro-apoptotic proteins. ATM did not seem to be involved in γH2AX activation. Co-incubation with catalase prevented the alterations elicited by *V. baccifera* in HepG2. Taking together, these results indicate that hydrogen peroxide mediates the HepG2 cytotoxic response and provide evidence for more in-depth studies of the signaling involved.

Keywords: Biochemistry, Cancer research, Cell biology, Molecular biology

https://doi.org/10.1016/j.heliyon.2018.e00675

## 1. Introduction

*Vismia baccifera* is a plant species of the Hypericaceae family, typically from the Amazonian rainforest. It is commonly used in traditional healing by indigenous populations. The folk medicine employs the preparation of macerations and decoctions of barks, leaves, stem, and roots of the plants with different curative purposes. *Vismia* was reported as an important purgative or for treating disorders of the urinary tract, and as an effective treatment for protecting against snake bites [1]. It is also used against skin diseases and as an antirheumatic and antipyretic [2]. The leaves of *V. baccifera* are recommended for a variety of inflammatory conditions, including uterine hemorrhage, as well as having leishmanicidal activity [3]. Other studies have shown antibacterial and anti-HIV activities of *Vismia* genus extracts [4].

For the development of new drugs, it is essential to identify natural products derived from plants that could be used as chemotherapeutic agents. Their use often avoids the side effects of synthetic drugs. To date no antitumor activity has been reported *in vivo* for *V. baccifera*. In the literature, a work described that an aqueous extract of *V. baccifera L. var. dealbata* leaf produced a moderate analgesic activity *in vivo* in experimental animals, similar to that found for acetylsalicylic acid, without causing toxicity at the concentration used [5]. One of the *V. baccifera* constituents, sesamin, was shown to inhibit the production of prostaglandins and the tumor necrosis factor $\alpha$, a molecule involved in inflammation [6]. Cancer and inflammation are closely related, since the proinflammatory prostaglandins generated from arachidonic acid play an important role in metastasis and proliferation in various cancer types, and in tumoral progression [7].

An important tool for cancer treatment is the induction of apoptosis in cancer cells. Hussein et al. [8] reported the *in vitro* cytotoxic effects of various methanolic extracts of leaves from plants belonging to the genus *Vismia* on human breast, lung and central nervous system cancer cell lines. In a previous work by our group an aqueous leaf extract of *V. baccifera* species was described [9]. The extract was rich in flavanols, particularly epicatechin (monomers, dimers and trimers), and flavonols. The plant infusion induced toxicity to human and rat hepatoma cell lines, increasing the intracellular levels of reactive oxygen species (ROS) at early times [10, 11]. Results suggested that the cell death could be mediated by ROS. In the present work we partially unravel the antitumor activity exerted by *V. baccifera* in the human hepatoma HepG2 cell line.

## 2. Materials and methods

### 2.1. Reagents

Amplex Red reagent, apocynin, N-acetyl-L-cysteine (NAC), catalase from bovine liver, 5,5′-dithiobis(2-nitrobenzoic acid) (DTNB), 4,5-dihydroxybenzene-1,3-disulfonic acid disodium salt monohydrate (Tiron), EGTA —ethylene glycol-bis(β-aminoethyl


https://doi.org/10.1016/j.heliyon.2018.e00675

ether)-N,N,N′,N′-tetraacetic acid—, (-)-epicatechin, L-glutamine, glutathione reductase, 4-hydroxypyrazolo[3,4-d]pyrimidine (allopurinol), (±)-6-hydroxy-2,5,7,8-tetramethylchromane-2-carboxylic acid (Trolox), 1-methyl-2-vinylpyridinium triflate (M2VP), NADPH, Nutrient Mixture F-12, Coon's modification (HAM F-12), propidium iodide, quercetin, streptomycin-penicillin solution, sulfosalicylic acid, superoxide dismutase (SOD), triethanolamine, Triton X-100, and trypsin were all obtained from Sigma-Aldrich (St Louis, MO, USA). 2′,7′-Dichlorodihydrofluorescein diacetate ($H_2$DCF-DA) was obtained from Molecular Probes (Eugene, OR, USA), dithiothreitol (DTT) and RNase A from Roche Biochemicals (Indianapolis, IN, USA). Ac-DEVD-AMC caspase-3 fluorogenic substrate was obtained from BD Pharmigen Biosciences (San Diego, CA, USA), crystal violet indicator from Merck (Darmstadt, Germany). Antibodies against the following proteins used Bax (sc-493V), Bcl-2 (sc-492), Bid (sc-11423), Bcl-$x_{L/S}$ (sc-634) and p21 (sc-6246) were purchased from Santa Cruz Biotechnology (Dallas, TX, USA), against Cu,Zn-SOD (574597) from Calbiochem (La Jolla, CA, USA), against Mn-SOD (06-984) from Millipore (Darmstadt, Germany), against poly(ADP-ribose) polymerase (PARP, #9542) from Cell Signaling Technology (Danvers, Massachusetts, USA), and against apoptosis-inducing factor (AIF, ab32516), p-ATM (ab81292), ATM (ab32420), p-γH2AX (ab22551), and GAPDH (ab8245) from Abcam (Cambridge, UK).

## 2.2. Preparation and characterization of the plant aqueous extract

The *V. baccifera* plant was collected from the forest of the Macagual Research Center in Florencia, Caquetá (Colombia). It was identified taxonomically by a botanical expert and deposited in the Herbarium of the Botanical Garden of the Amazonia University-HUAZ (Florence, Colombia). The plant samples were processed in the laboratory within a maximum of 24 h after harvesting. Otherwise, the material was stored under refrigeration at 4 °C. The aqueous leaf extract of *V. baccifera* was prepared from infusions, as it has been described [12]. The samples were carried to the Physiology Department at the Medicine and Nursing School of the University of the Basque Country UPV/EHU (Spain). Once defrosted, samples were centrifuged at 1,200 g for 5 min at 4 °C, sterilized by filtration, and aliquots of supernatants were frozen at −80 °C. One gram of dry weight of the *V. baccifera* extract corresponded to 10 grams of fresh plant leaves.

## 2.3. Cell cultures

The human hepatoma cell line HepG2 and the human fetal hepatocyte-derived HH4 cell line were purchased from ATTC (Manassas, USA). HepG2 were maintained in 75 $cm^2$ flasks in Eagle's Minimum Essential Medium supplemented with 10% heat inactivated fetal bovine serum (FBS) plus 2 mM L-glutamine, 0.1 mg/ml streptomycin and 100 U/ml penicillin. HH4 cell line was maintained in HAM F-12 containing 15% heat inactivated FBS, 0.1 mg/ml streptomycin, 100 U/ml penicillin and


https://doi.org/10.1016/j.heliyon.2018.e00675

32 mM sodium bicarbonate. Cells were grown at 37 °C in humidified atmosphere with 5% $CO_2$ under 21% $pO_2$. Medium was replaced every 3 days. Confluent cells were detached with a solution of 0.1% trypsin-0.04% NaEDTA and then harvested to perform subsequent experiments. The cells were then seeded in the corresponding plates to perform subsequent experiments. After adaptation, cells were incubated without (control) or with *V. baccifera* for different times. When the effect of antioxidants was studied, the compounds were added one hour before the addition of the extract. When it is not specified in the figures, the concentrations used in the assays were 75 μg/ml *V. baccifera*, 10 kU/ml catalase, 1 mM NAC, 100 μM Trolox, 1 mM Tiron, 100 μM allopurinol, and 300 μM apocynin.

## 2.4. Cytotoxicity assay

The live cell number was evaluated with the crystal violet assay, as described previously [11].

## 2.5. Intracellular ROS

Intracellular ROS levels were measured using the cell-permeant 2′,7′-dichlorodihydrofluorescein diacetate ($H_2$DCF-DA) probe, as described in [11]. Inside the cells, the probe is deacetylated and oxidized forming the fluorescent compound, 2′,7′-dichlorofluorescein (DCF).

## 2.6. Hydrogen peroxide measurement

Hydrogen peroxide ($H_2O_2$) was determined in the culture medium using Amplex Red. In the presence of horseradish peroxidase (HRP), the Amplex Red reagent reacts with $H_2O_2$ to produce highly fluorescent resorufin. Measurements were done in 96-well plates, where $5 \times 10^3$ cells per well were seeded. After treatment, the cells were washed with PBS at 37 °C and the reaction was started by the addition of 0.1 U/ml of HRP and 50 μM Amplex Red in Krebs-Ringer phosphate buffer (145 mM NaCl, 5.7 mM $Na_2HPO_4$, 4.86 mM KCl, 0.54 mM $CaCl_2$, 1.22 mM $MgSO_4$, 5.5 mM glucose, pH 7.35). A standard curve was prepared using commercially $H_2O_2$ (0.42−1.7 μM). Fluorescent variations were determined by continuous recording of the fluorescence ($\lambda_{exc}$ = 538 nm, $\lambda_{em}$ = 604 nm) at 37 °C for 2 h at 5 min intervals in a Synergy HT fluorometer microplate reader (BioTeck, Winooski, VT, USA). The $H_2O_2$ concentration was determined by subtracting the fluorescence remaining in sample wells after the addition of catalase (10 U/well). Fluorescent changes from the $H_2O_2$ release from cells were converted to nmol $H_2O_2$/mg protein using the $H_2O_2$ standard curve.

## 2.7. Determination of glutathione

Glutathione (GSH) was evaluated with the glutathione reductase-DTNB recycling method, as reported previously [11].


https://doi.org/10.1016/j.heliyon.2018.e00675

## 2.8. Enzymatic assays

After treatments, cells were lysed by freeze-thawing in liquid $N_2$. Samples were centrifuged at 16,000×g for 10 min at 4 °C, and the antioxidant activities were measured in the supernatant. Total protein was quantified by Coomassie Blue dying [13].

### *2.8.1. Superoxide dismutase activity (EC 1.15.1.1)*

SOD activity was determined indirectly by the method of nitroblue tetrazolium, as is described in [11].

### *2.8.2. Glutathione peroxidase (EC 1.11.1.9)*

Total glutathione peroxidase (GPx) activity was assayed by the indirect method of Flohé & Güntzler [14]. The decrease in absorbance of NADPH was monitored at 340 nm every 60 sec for 15 min in a 96-well plate reader at 30 °C. The final volume was 225 μl containing 50 mM potassium phosphate buffer (pH 7.0), 1 mM EDTA-$Na_2$, 0.5 mM sodium azide, 0.45 mM GSH, 0.2 mM NADPH and 0.45 U of glutathione reductase. The reaction started by the addition of cumene hydroperoxide (0.72 mM). The results are expressed as nmol/min/mg of protein, using the NADPH experimental coefficient $\varepsilon = 3.065\ mM^{-1}$.

## 2.9. Cell cycle analysis

Cells were seeded at a density of $2.5 \times 10^5$ cells onto 6-well plates. After treatment, no-adherent and adherent cells were harvested and fixed in 70% ice-cold ethanol overnight at 4 °C. After washing with ice-cold PBS, cells were stained with a 25 μg/ml propidium iodide solution containing 200 μg/ml RNase A for 45 min at 37 °C in the dark. The cell cycle distribution of the cells was determined by flow cytometry in a Beckman Coulter Gallios Flow Cytometer in SGIker of the UPV/EHU with a total acquisition of 10,000 events. The distribution of cells in different phases of the cell cycle was analyzed by Summit 4.3 software (Dako, Hovedstaden, Denmark).

## 2.10. Caspase-3 activity

HepG2 were seeded at a density of $1 \times 10^6$ cells onto Petri dishes for 72 h before starting the experiment. After treatment for 24 h, cells were washed with ice-cold PBS and resuspended in ice-cold lysis buffer (1 mM NaF, 10 mM EGTA, 40 mM β-glycerol phosphate, 1% NP-40, 2.5 mM $MgCl_2$, 2 mM orthovanadate, 1 mM DTT, 10 μg/ml protease inhibitor cocktail, and 20 mM Hepes, pH 7.5) for 30 min on ice. Cell extracts were centrifuged at 16,000×g for 10 min at 4 °C. The caspase-3 activity was carried out using specific Ac-DEVD-AMC fluorogenic


https://doi.org/10.1016/j.heliyon.2018.e00675

substrate. The reaction mixture contained 50 μg of cell protein in assay medium (200 mM NaCl, 0.2 % CHAPS, 2 mM EDTA, 20 % glycerol, 5 mM DTT, 100 mM Hepes, pH 7.4) and 37 μM Ac-DEVD-AMC. The activity was determined by continuous recording of the released AMC ($\lambda_{exc} = 360$ nm, $\lambda_{em} = 460$ nm) at 37 °C for 2 h every 5 min in a Synergy HT fluorometer microplate reader.

## 2.11. Protein immunodetection

Cu,Zn-SOD, Mn-SOD, p21, PARP, Bax, Bcl-2, Bid and Bcl-$x_{L/S}$, p-ATM, ATM, p-γH2AX and GAPDH were detected by western blot. Cellular protein extracts were boiled at 95 °C for 5 min in Laemmli buffer [15] and separated by SDS-PAGE electrophoresis in 11−15% polyacrylamide gels. Gels were transferred onto PVDF membranes by electroblotting with constant amperage (1 mA/cm$^2$). After blocking for 1 h at room temperature, membranes were incubated overnight at 4 °C with the corresponding primary antibody (anti-Cu,Zn-SOD 1:7000, anti-Mn-SOD 1:2000, anti-p21 1:500, anti-PARP 1:1000, anti-p-ATM 1:7000, anti-ATM 1:5000, anti-p-γH2AX 1:1000, and anti-GAPDH 1:10000, and anti-Bax, anti-Bcl-2, anti-Bid and anti-Bcl-$x_{L/S}$ 1:500). After washing, membranes were probed with the secondary antibody conjugated to horseradish peroxidase for 1 h. The immunoreactive proteins were detected with the Clarity Western ECL substrate (Bio-Rad, Hercules, California, USA) and the blots were imaged by scanning with the C-DiGit LI-COR blot scanner (Bonsai Advanced technologies S.L., Madrid, Spain). GAPDH was used as the loading control.

To characterize mass expression of SOD isoforms, a standard curve (6.6−33 ng Cu,Zn-SOD and 1.6−7.9 ng Mn-SOD) was prepared using commercial human recombinant SOD proteins (ProSpec-Tany TechnoGene Ltd., Israel). Values were interpolated in the linear range of the standard curve.

## 2.12. Immunofluorescence confocal microscopy

The subcellular localization of AIF was analyzed by immunocytochemistry. HepG2 cells were plated on coverslips and incubated with the plant extract for 24 h. After treatment, HepG2 cells were stained with MitoTracker Red (500 nM) for 30 min at 37 °C to detect the mitochondria. Afterwards, the cells were fixed in 4% formaldehyde, washed with PBS and permeabilized with 0.05% Triton X-100 in TBS 10 mM (pH 7.4), and blocked with 1% preimmune goat serum/1% BSA for 1 h at room temperature. Then, the cells were incubated overnight with anti-AIF 1:100, washed and incubated for 1 h with secondary antibody Alexa Fluor 488 conjugated goat anti-rabbit (ThermoFisher scientific, Walthan, Massachusetts, USA). Nuclei were stained using 5 μg/ml DAPI. Images were obtained with an Olympus Fluoview FV500 confocal microscope (Olympus, Tokyo, Japan) at the Analytical Microscopy Service in the General Research Services SGIker of the UPV/EHU.


https://doi.org/10.1016/j.heliyon.2018.e00675

## 2.13. Statistical analysis

The statistical package SPSS 19.0 (SPSS Inc., Chicago, IL, USA) was used for data analysis. The results were expressed as mean ± standard error (SE) from at least three experiments. Statistical significance for the differences of the means was estimated by parametric Student's t-test or non-parametric Wilcoxon test, depending on the sample distributions, for paired data. Differences between means were considered statistically significant if $P < 0.05$.

# 3. Results

## 3.1. *V. baccifera* does not induce toxicity to nontransformed HH4 hepatocytes and its major monomeric flavonoid constituents alone are not responsible of the induced toxicity to HepG2

The *V. baccifera* extract used in this work was toxic to HepG2 with an IC50 of 45 μg/ml, and also increased intracellular ROS in a time-dependent manner [11]. In nontransformed HH4 lines derived from immortalized human fetal hepatocytes the extract (concentrations up to 150 μg/ml) did not affect viability (Fig. 1A). As regards intracellular ROS, only an occasional increase of DCF fluorescence was detected at 1 h of exposure (Fig. 1B).

(-)-Epicatechin (concentrations up to 100 μM) did not decrease HepG2 cell growth (Fig. 1C). On the other hand, quercetin monomer induced significant cell toxicity at

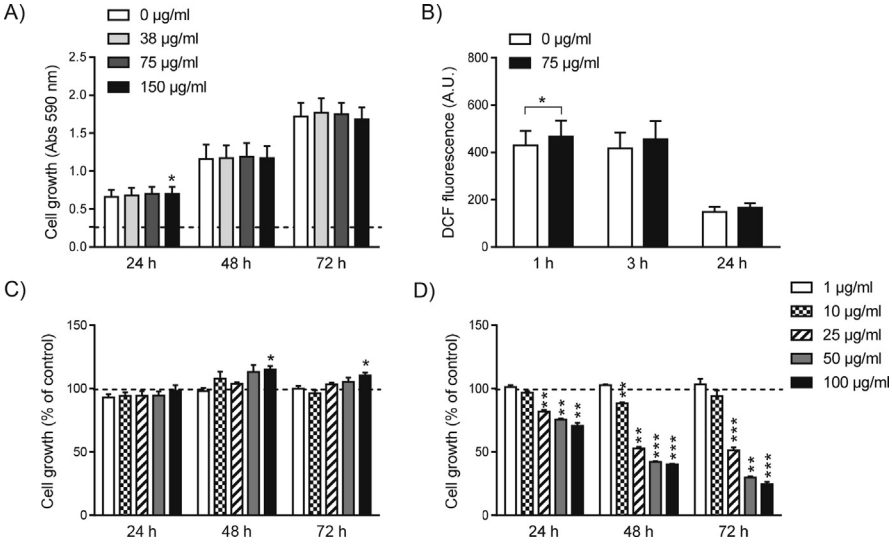


**Fig. 1.** *V. baccifera* does not induce toxicity to nontransformed HH4 cells and they major monomeric flavonoid components are not responsible of its toxicity to HepG2. (A) Cell growth and (B) intracellular ROS accumulation in HH4 cells exposed to *V. baccifera*. In (A) the absorbance of the control at time zero was 0.264 at 590 nm, and is represented as a dashed line. (C) Effect of (-)-epicatechin and (D) quercetin monomers on HepG2 cell growth. Cells were incubated with increasing concentrations (1−100 μg/ml) of the flavonoids at the indicated times. Results are expressed as the percentage of the control values, represented as a dashed line. *P < 0.05, **P < 0.01, ***P < 0.001 vs control at the same time.


https://doi.org/10.1016/j.heliyon.2018.e00675

concentrations higher than 10 μM (Fig. 1D). These quantities are incompatible with quercetin concentrations in the extract, which are at least an order of magnitude lower [10].

## 3.2. ROS, particularly $H_2O_2$ and $O_2^-$, are involved in *V. baccifera*-induced toxicity to HepG2

To evaluate whether ROS was a significant factor in the plant-induced cytotoxicity and to elucidate the source/nature of ROS, different free radical scavengers (catalase, NAC, Trolox and Tiron), and inhibitors of xanthine oxidase (allopurinol) and NADPH oxidase (apocynin) were examined. Catalase completely prevented *V. baccifera*-induced toxicity (Fig. 2A). The enzyme even increased cell growth at 24 h. Catalase also decreased ROS accumulation from 3 h and completely prevented the ROS increase at 24 h (Fig. 2B). The $O_2^-$ scavenger Tiron partially reverted the decrease in the cell number (9% at 48 h) and significantly reduced ROS levels at all times. The cytotoxic response to the extract was unaffected by co-exposure

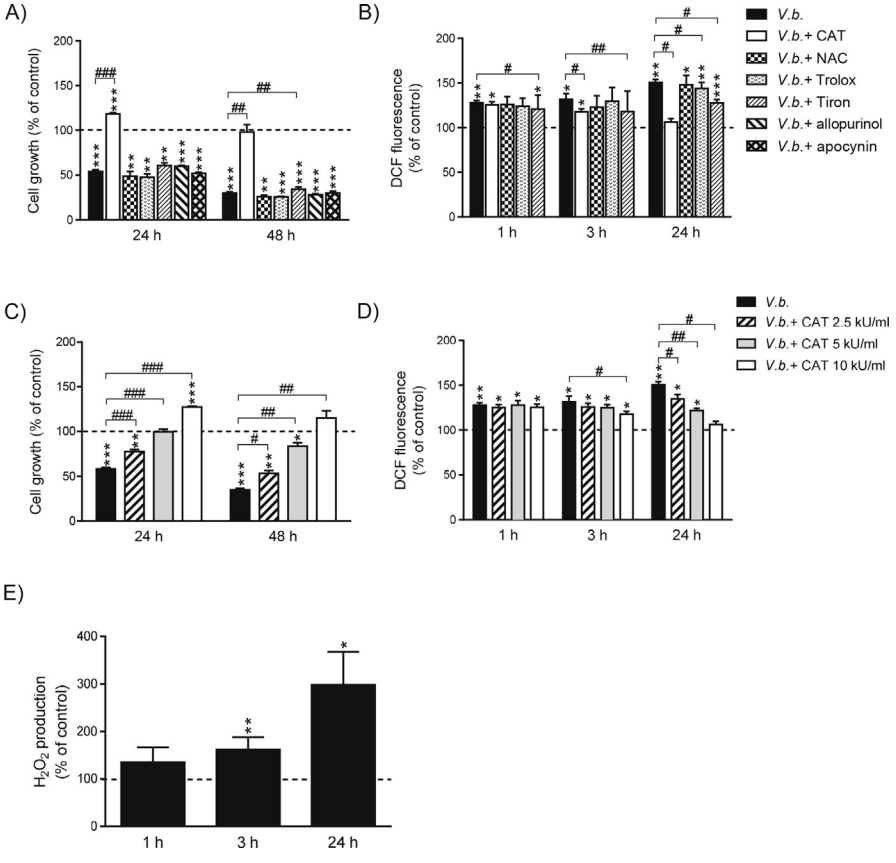


**Fig. 2.** Hydrogen peroxide and to a lesser extent $O_2^-$ are involved in *V. baccifera*-induced totoxicity and ROS formation in HepG2. (A−D) Cells were incubated without (control) and with *V. baccifera* either alone or with the indicated compounds. After treatments, cell growth and DCF fluorescence were measured as described in Materials and Methods. E) Cells were incubated without and with *V. baccifera*. After incubation, the medium was used to determine $H_2O_2$ by Amplex Red. Results are the mean + SE from 5 experiments. *P < 0.05, **P < 0.01, ***P < 0.001 vs control at the same time. #P < 0.05, ##P < 0.01, ###P < 0.001 vs *V. baccifera*. CAT, catalase; NAC, N-acetyl-L-cysteine.


https://doi.org/10.1016/j.heliyon.2018.e00675

with NAC, Trolox, allopurinol, and apocynin, although the peroxyl radical scavenger Trolox slightly decreased ROS at 24 h. The exposure to catalase protected the cells dose- and time-dependently (Fig. 2C). At 10 kU/ml catalase even increased cell growth. As regards ROS, catalase dose-dependently decreased its accumulation at 24 h (Fig. 3D). This effect on intracellular ROS was observed as early as 3 h for the highest concentration of catalase.

The $H_2O_2$ production inside the cells can be estimated by measuring the $H_2O_2$ released to the medium, since this molecule freely crosses the plasma membrane. *V. baccifera* significantly increased the rate of $H_2O_2$ production from 3 h, as was detected by the Amplex Red specific probe for $H_2O_2$ (Fig. 2E).

## 3.3. Catalase prevents *V. baccifera*-induced oxidative stress in HepG2

*V. baccifera* induced a significant increase of SOD activity (35%) and concomitantly decreased GPx activity, as well as the intracellular GSH levels (Fig. 3).

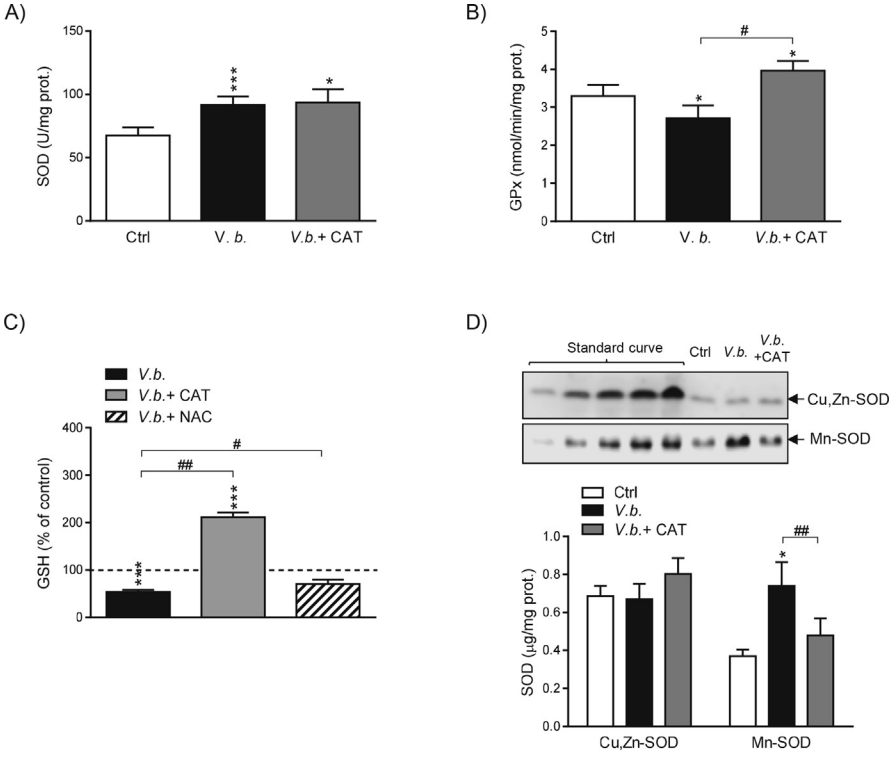


**Fig. 3.** *V. baccifera* induces changes in antioxidant enzymes tending to accumulate $H_2O_2$ and reduces GSH levels. Cells were incubated for 24 h without (control, Ctrl) and with *V. baccifera* alone or plus catalase or NAC. (A) SOD activity. (B) GPx activity. (C) Intracellular GSH. GSH is expressed as the percentage of the control value, which was 40 ng GSH/mg protein and is represented as a dashed line. (D) Expression of Cu,Zn-SOD and Mn-SOD isoforms by western blotting. Human recombinant proteins were used to construct a standard curve to quantify absolute amounts of Cu,Zn-SOD and Mn-SOD. The bands are representative of at least four experiments (Supplementary Fig. 3). $^{*}P < 0.05$, $^{***}P < 0.001$ *vs* control. $^{\#}P < 0.05$, $^{\#\#}P < 0.01$, $^{\#\#\#}P < 0.01$ *vs V. baccifera*. CAT, catalase; NAC, N-acetyl-cystein.


https://doi.org/10.1016/j.heliyon.2018.e00675

Co-incubation with catalase increased both GPx activity and GSH above control values. Nevertheless, it did not affect SOD activity. NAC, despite not preventing toxicity to HepG2 (Fig. 2A), reverted GSH to control levels (Fig. 3D), thus suggesting that the decrease in GSH is not critical to the toxic effect of the extract.

As regards SOD expression, under basal conditions the cytosolic protein (Cu,Zn-SOD) was almost two-fold higher expressed than the mitochondrial isoform (Mn-SOD) (Fig. 3D). *V. baccifera* did not affect Cu,Zn-SOD expression, but dramatically increased the levels of Mn-SOD. The addition of exogenous catalase reduced the amount of Mn-SOD to control values. Our results suggest that $H_2O_2$ is involved in the regulation of GPx activity and the expression of Mn-SOD, while the changes in SOD activity are independent of $H_2O_2$.

## 3.4. Catalase prevents *V. baccifera*-induced cell cycle arrest in HepG2

*V. baccifera* markedly increased the number of cells in subG0 ($P < 0.001$, Fig. 4A). The extract also increased by 24% the number of cells in G2/M and reduced by 40% the number of cells undergoing DNA replication (S-phase, $P < 0.01$). Catalase significantly decreased the number of cells in subG0 and completely prevented cell cycle arrest. The extract activated p21, an inhibitor protein of the cyclin-dependent kinase (CDK), its expression being near 2.5-fold higher than the control value along the time studied (Fig. 4B). The co-incubation with catalase completely prevented p21 activation during the first 6 h, reinforcing the role of ROS in the cell cycle arrest by *V. baccifera*.

## 3.5. Catalase prevents *V. baccifera*-induced apoptosis of HepG2

The extract activated caspase-3 as early as 3 h ($P < 0.01$), with the activity being 3.5-fold higher than the control value at 24 h (Fig. 5A). Commercial catalase completely prevented caspase-3 activation. The plant also increased PARP processing by caspase-3 and catalase inhibited PARP cleavage (Fig. 5B). As regards the Bcl-2 family proteins, *V. baccifera* triggered a significant increase of the pro-apoptotic Bax and reduced the anti-apoptotic Bcl-2 expression at 24 h, thus increasing the ratio of Bax to Bcl-2 (Fig. 5C). Co-incubation with catalase prevented the Bcl-2 decrease, thus resulting in a lower Bax/Bcl-2 ratio. The extract also increased the apoptotic Bid protein and concomitantly reduced the expression of anti-apoptotic Bcl-$x_L$ at 24 h. The almost 6-fold increase of the Bid to Bcl-$x_L$ ratio was completely prevented by catalase.

## 3.6. Catalase prevents *V. baccifera*-induced DNA damage by an ATM-independent pathway

AIF is a mitochondrial intermembrane protein that after apoptosis translocates into the nucleus, triggering chromatin condensation and DNA fragmentation [16]. To


https://doi.org/10.1016/j.heliyon.2018.e00675

A)

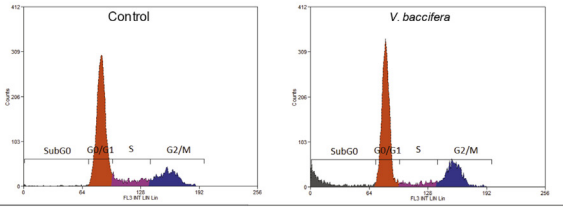


| | Cells in cell cycle | | | |
|---|---|---|---|---|
| | SubG$_0$ (%) | G$_0$/G$_1$ (%) | S (%) | G$_2$/M |
| Control | 1.6 ± 0.2 | 67.9 ± 1.0 | 13.2 ± 0.7 | 18.8 ± 0.4 |
| *V. baccifera* | 11.7 ± 0.7*** | 68.9 ± 0.6 | 7.9 ± 0.4** | 23.4 ± 0.8** |
| *V. baccifera* + CAT | 2.9 ± 0.3**, ### | 67.8 ± 0.7 | 12.7 ± 0.5# | 19.5 ± 0.4# |

B)

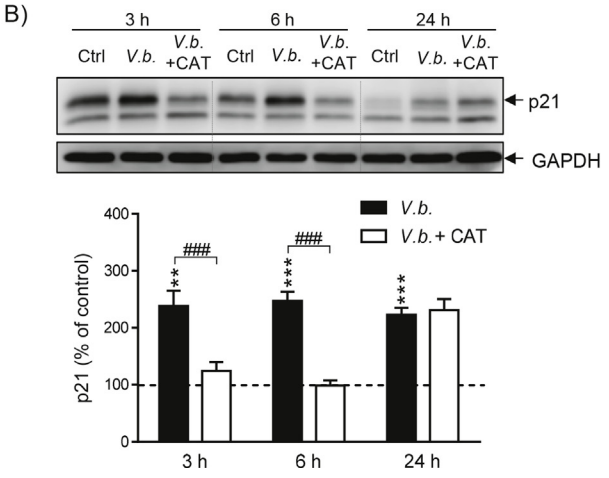


**Fig. 4.** Catalase prevents *V. baccifera*-induced cell cycle arrest. Cells were incubated for 24 h (flow cytometry assays) or the indicated times without (control, Ctrl) and with *V. baccifera* either alone or with catalase. (A) Flow cytometry analysis. Cells in subG0 phase were expressed as the percentage of the total cells (SubG0 + G0/G1 + S + G2/M). B) Expression of the CDK inhibitor, p21 protein. The bands shown are representative of 6 experiments. Results are the mean + SE of the densitometry changes from the western blots (Supplementary Fig. 4). $^{**}P < 0.01$, $^{***}P < 0.001$ *vs* control. $^{\#}P < 0.05$, $^{\#\#}P < 0.01$, $^{\#\#\#}P < 0.001$ *vs V. baccifera*. CAT, catalase.

study AIF mobilization, live cells were stained for the detection of mitochondria using the MitoTracker probe. AIF in control cells was mainly located in mitochondria and virtually absent in the nucleus (Fig. 6A). *V. baccifera* induced the nuclear translocation of AIF at 24 h, not affecting the protein location at early times (data not shown).

One of the major signaling pathways activated by DNA damage consists of the ATM-Chk1 protein kinases [17], mainly activated by double-stranded DNA breaks. Following the initial activation of ATM by DNA damage, ATM phosphorylates the histone γH2AX. Immunoblotting was used to determine whether the ATM/γH2AX


https://doi.org/10.1016/j.heliyon.2018.e00675

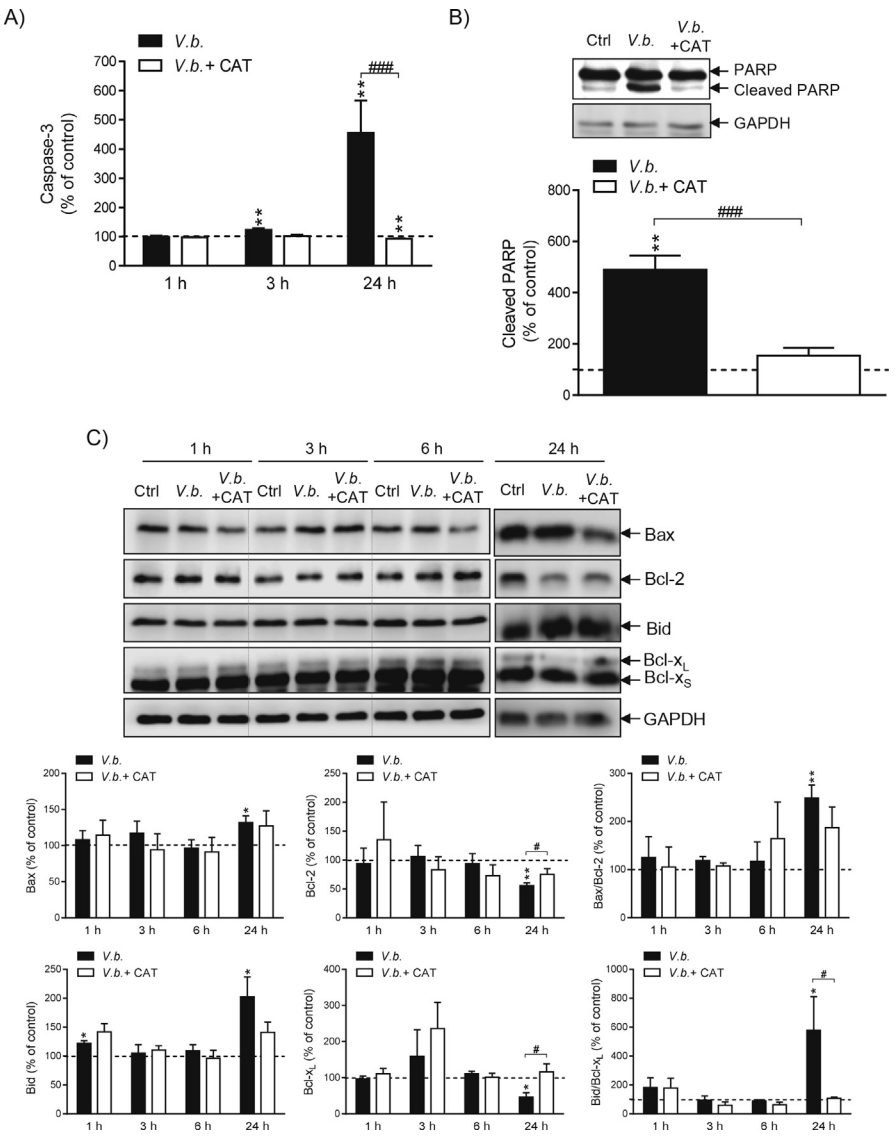


**Fig. 5.** Catalase prevents *V. baccifera-induced* apoptosis in HepG2. Cells were incubated for 24 h or the indicated times without (control, Ctrl) and with *V. baccifera* either alone or with catalase. (A) Caspase-3 activity. (B) Cleaved PARP. (C) Expression of the Bcl-2 family proteins. The bands shown are representative of at least 3 experiments (Supplementary Fig. 5). The densitometry changes from the western blot experiments are expressed as the percentage of the control values. $^{*}P < 0.05$, $^{**}P < 0.01$ *vs* control. $^{\#}P < 0.05$, $^{\#\#\#}P < 0.001$ *vs V. baccifera*. CAT, catalase.

pathway was activated by the extract. The phospho-ATM protein increased with the treatment (Fig. 6B). In the presence of catalase p-ATM levels were even higher. On the other hand, there was a sharp increase in γH2AX phosphorylation, which was amelliorated by catalase (Fig. 6C). Thus, these results indicate that ATM pathway does not promote the γH2AX activation. In this respect, γH2AX can also be activated by ATR pathway [18]. Together, these data suggest that *V. baccifera* induces


https://doi.org/10.1016/j.heliyon.2018.e00675

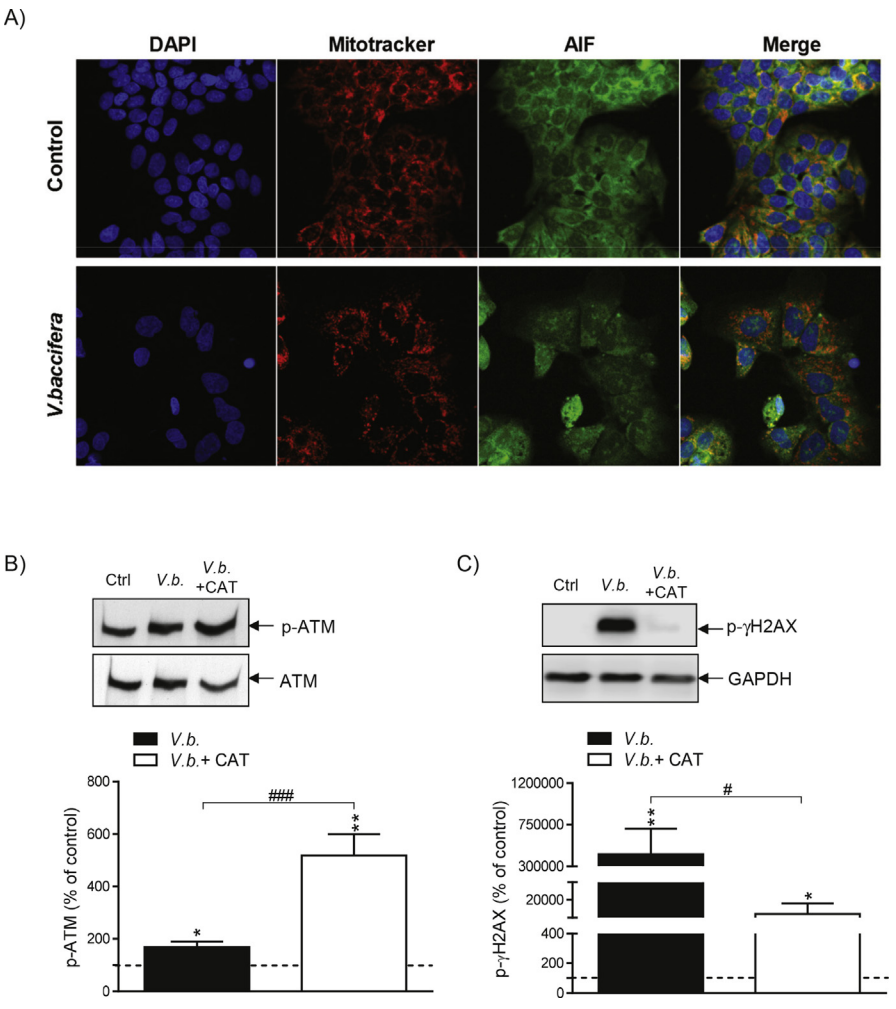


**Fig. 6.** Catalase prevents *V. baccifera*-induced DNA damage by an ATM-independent pathway. (A) After treatment for 24 h, cells were stained with MitoTracker Red to detect the mitochondria (red), and specific AIF antibody (green). B) ATM phosphorylation and (C) γH2AX phosphorylation in HepG2 treated with *V. baccifera* either alone or with catalase. The bands shown are representative of at least 3 independent experiments. Results are the mean + SE from 3-6 experiments and are expressed as the percentage of the control values (Supplementary Fig. 6). $^{*}P < 0.05$ and $^{**}P < 0.01$ *vs* control. $^{\#}P < 0.05$ *vs V. baccifera*. CAT, catalase.

DNA damage, with γH2AX being activated by $H_2O_2$ independently of ATM kinase in a process where $H_2O_2$ has a role.

## 4. Discussion

In this work, we unravel the mechanism of the *in vitro* antitumor action of an aqueous leaf extract of *V. baccifera* against the human hepatocarcinoma HepG2 cell line. The extract inhibited cell proliferation and also strongly increased both the mitochondrial $O_2^-$ and the intracellular ROS levels at early time points [11]. It should be pointed out that the plant did not cause considerable changes in either


https://doi.org/10.1016/j.heliyon.2018.e00675

viability or ROS accumulation in HH4 cells, the non-transformed human fetal hepatocyte line, thus indicating that the cytotoxic actions are restricted to tumor cells.

The aqueous extract of *V. baccifera* leaves was rich in flavonoids, particularly (-)-epicatechin monomers dimers and trimers, and quercetin [10]. Flavanols from green tea (epicatechin derivatives among them) exert antitumor activities *in vitro*, and are also associated with antitumor properties *in vivo* [19]. In our study the main (-)-epicatechin flavanol component was unable to stop cell proliferation or induce toxicity to HepG2, thus excluding this constituent as responsible for the antitumor action of *V. baccifera*. It is not ruled out, however, that flavanol oligomers could cause toxicity. Some studies suggest that the oligomer chain length of polymerized oligomers of (-)-epicatechin may be a critical factor determining the pro-apoptotic effects of procyanidins. Thus, only flavanol oligomers and polymers, but not monomers or dimers, increased apoptosis of esophageal adenocarcinoma cells [20].

We investigated the source of ROS. NADPH oxidases (NOXs) are intracellular free radical generators that are expressed in several tissues in different subcellular locations. The enzyme complex produces $O_2^-$/ROS, and the NOX-generated free radicals are involved in cellular functions, such as intracellular signaling of cell proliferation and differentiation [21]. A cancer-specific NOX protein, called tNOX, was also identified in the surface of cancer cells. It is absent in normal cells, and has been considered as a target for cancer therapies [22]. There are controversies in the literature regarding the role of polyphenols in NOX regulation. On the one hand, various polyphenols inhibited NOX activity in several tissues [23], and naturally occurring polyphenols, such as catechin (-)-epigallocatechin gallate and vanilloid capsaicin, inhibited tNOX, producing cell death [24]. On the other hand, several polyphenolic compounds, particularly phenolic acids, induced apoptosis in HepG2, and the ROS generated through the activation of NOX were responsible for the apoptotic response [25]. In our study, the apocynin NOX inhibitor was unable to prevent toxicity. This enzyme therefore, does not seem to be involved in the mechanism of action of *V. baccifera*.

Xanthine oxidase, an $H_2O_2$-generating enzyme, did not appear to mediate cell toxicity, since allopurinol had a null effect on cells treated with *V. baccifera*. Recently, it has been reported that $H_2O_2$ generated by xanthine oxidase did not cause, but was rather the result of cell death in various cancer cell types [26].

Trolox, a lipid peroxyl radical scavenger, was unable to prevent cell growth inhibition, although partially reduced ROS increase. Thus, these type of free radicals derived from polyunsaturated fatty acids did not have a central role in the toxic mechanism of action. Among the different antioxidants used, only the $O_2^-$ scavenger Tiron, and the $H_2O_2$ eliminating enzyme catalase were effective in reducing cell toxicity. Tiron partially reduced the decrease in the cell number, suggesting that $O_2^-$ could be involved in the inhibition of cell growth. It was noteworthy that Tiron


https://doi.org/10.1016/j.heliyon.2018.e00675

was toxic in a dose- and time-dependent manner, and higher concentrations of the compound could not be used in the assay, thus limiting the study of its protective effect (data not shown).

One of the defense systems against oxidative stress involves glutathione. GSH is the major non-protein thiol source that functions as a sulfhydryl buffer inside the cells. Its levels are tightly controlled for proper cellular function [27]. Depletion of GSH involves increases in ROS and, inversely, a ROS increase often leads to GSH depletion and alterations in the redox balance. The *in vitro* addition of NAC to HepG2 prevents toxicity triggered by pro-oxidant stimuli [28]. NAC is a thiol-containing compound that acts as a sulfide source, necessary in glutathione synthesis. Inside the cell, it is readily deacetylated to yield L-cysteine, functioning as a GSH precursor. NAC has also been applied *in vivo* to diseases associated with oxidative stress [29] and against cancer, acting as adjuvant that reduces the chemotherapy-related toxicity [30]. In our system, NAC was unable to protect cells against toxicity, despite it prevented GSH depletion. These results suggest that GSH depletion is not the cause of the observed cytotoxicity, but rather the consequence of an initial oxidative stress generated by the extract. Moreover, the thiol containing antioxidant was unable to prevent ROS accumulation, which suggests that free radicals could trigger the cytotoxic response. Furthermore, $H_2O_2$ production detected by a specific probe increased after 3 h of treatment, supporting the $H_2O_2$ cell origin.

On the other hand, we also analyzed the antioxidant enzyme status in HepG2. Our results showed that *V. baccifera* decreased GPx activity and increased Mn-SOD expression and SOD activity, but did not modify Cu,Zn-SOD expression. The up-regulation of SOD and reduction of GPx would result in the elevation of $H_2O_2$ inside the cells, thus triggering the cytotoxic response. Indeed, our results are in accordance to the study of Khan et al. [31], where resveratrol, a phenolic phytochemical present in vegetables and red wine, up-regulated Mn-SOD expression, not affecting Cu,Zn-SOD, and increasing SOD activity, inducing $H_2O_2$ accumulation in prostate, hepatic, and breast tumor cell lines.

The cell cycle arrest underlies apoptotic cell death. Many cancer cells have a defective G1 checkpoint, resulting in a higher dependence on the G2 checkpoint. DNA damage during cell replication is one of the main reasons for arresting at G2 phase; therefore, the G2 checkpoint is considered as a specific target for anticancer therapy [32]. *V. baccifera* blocked cell cycle selectively at G2/M phase in HepG2, which might be the result of the observed drastic activation of γH2AX, which is rapidly expressed after DNA damage [12]. Moreover, AIF and γH2AX interact directly in the nucleus with high affinity to mediate cell death [33]. On the other hand, *V. baccifera* also promoted the accumulation of CDK inhibitor p21, which can be activated during the G2 cell cycle arrest. It has been reported that genistein and


https://doi.org/10.1016/j.heliyon.2018.e00675

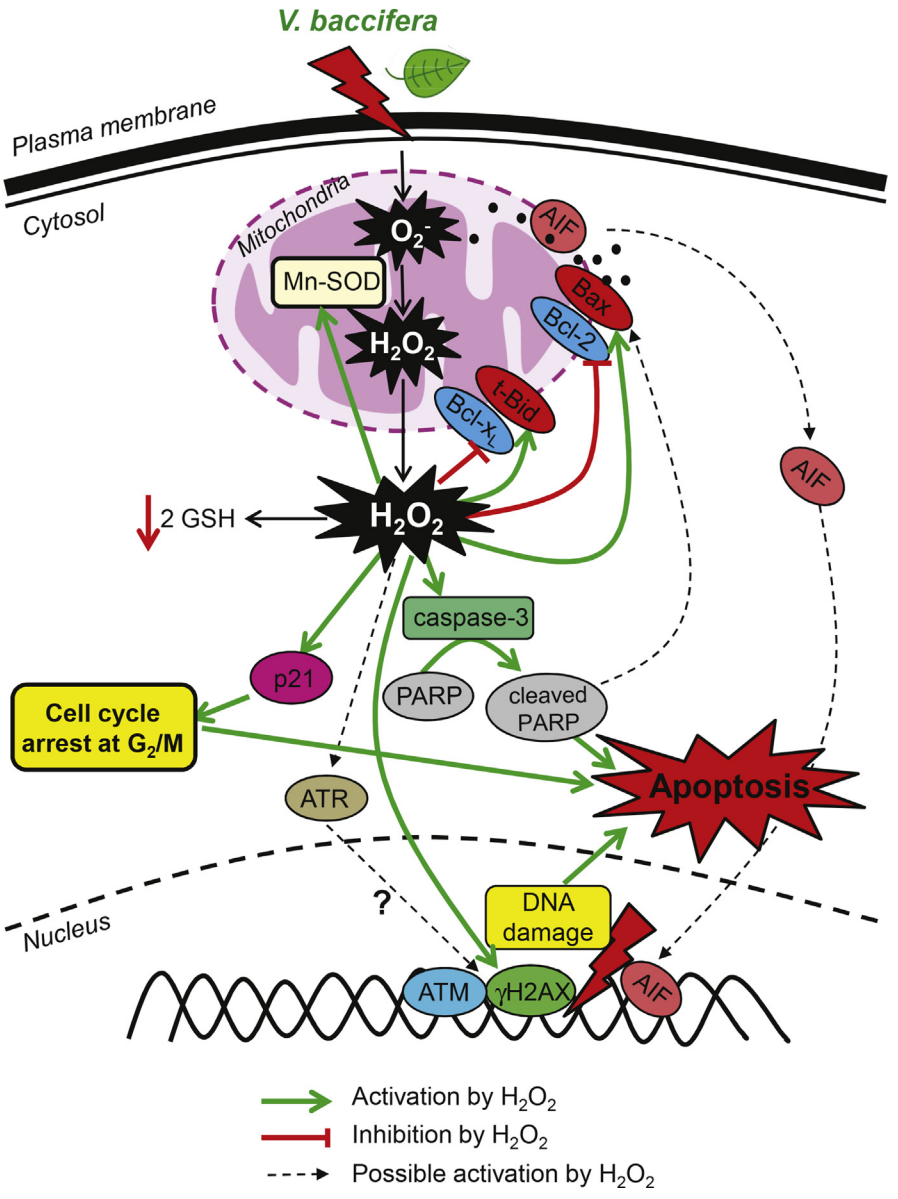


**Fig. 7.** Proposed mechanism of action elicited by *V. baccifera* in HepG2 cells.

theaflavins, the major components of black tea, affect the expression of proteins that regulate G2/M transition in several human cancer cell lines [34].

In light of the role of $H_2O_2$ in the toxicity induced by *V. baccifera* in HepG2, we detected an accumulation of the pro-apoptotic Bax and Bid proteins. Induction of the apoptotic pathway was confirmed with the caspase-3 activation and PARP cleavage. The $H_2O_2$ scavenger catalase completely prevented ROS formation, cell toxicity, as well as apoptosis. These results indicate how the increase in intracellular ROS is essential to induce apoptosis after exposure of HepG2 cells to *V. baccifera*, and support a role for $H_2O_2$ in the apoptotic process triggered by the plant.


https://doi.org/10.1016/j.heliyon.2018.e00675

In summary, the present study shows that *V. baccifera* induces in human hepatocarcinoma HepG2 cells accumulation of intracellular ROS and mitochondrial $O_2^-$, deregulation of antioxidant enzymes, cell cycle arrest at G2/M, DNA damage, and activation of pro-apoptotic proteins. Intracellular ROS, particularly $H_2O_2$, seem to be responsible of the cytotoxic response to the extract. According to our results and the bibliography, we propose the *V. baccifera*-induced signaling mechanism depicted in Fig. 7. The in-depth study of the mechanisms underlying the antitumor response to the plant and the use of *in vivo* animal models will help to better understand the potential application of this species as therapeutic agent in the management of liver cancer.

## Declarations

## Author contribution statement

Jenifer Trepiana: Conceived and designed the experiments; Performed the experiments; Analyzed and interpreted the data; Contributed reagents, materials, analysis tools or data; Wrote the paper.

M. Begoña Ruiz-Larrea: Conceived and designed the experiments; Analyzed and interpreted the data; Contributed reagents, materials, analysis tools or data; Wrote the paper.

José Ignacio Ruiz-Sanz: Conceived and designed the experiments; Performed the experiments; Analyzed and interpreted the data; Contributed reagents, materials, analysis tools or data.

## Funding statement

This work was supported by the Basque Government (ref. IT687-13), and University of the Basque Country UPV/EHU (CLUMBER UFI11/20, and pre-doctoral and post-doctoral grants to J.T.).

## Competing interest statement

The authors declare no conflict of interest.

## Additional information

Supplementary content related to this article has been published online at https://doi.org/10.1016/j.heliyon.2018.e00675.

## Acknowledgements

We thank Leandro J. Lizcano (University of Amazonia, Florencia, Colombia) for collecting the plant and characterizing the extract. We are grateful to José Antonio

López for his skillful technical assistance. Technical and human support provided by SGIKer (UPV/EHU, MICINN, GV/EJ, ESF) is gratefully acknowledged.

## References

[1] J. Ewan, Synopsis of the South Smerican Species of Vismia (Guttiferae), vol. 35, 1962, pp. 293–377.

[2] E. Pérez-Arbeláez, Plantas útiles de Colombia, fourth ed, vol. 752, Litografía Arco, Bogotá, 1978.

[3] A. Gallego, F. Torres, S. Robledo, I.D. Vélez, L. Carrillo, D.L. Muñoz, W. Quiñones, R. Fonnegra, J. Roldán, L. Valencia, O. Triana, F. Echeverri, Leishmanicidal and trypanocidal activity of Acacia farmesiana, Piper aierianum, P. subpedale, Sphagnum recurvum, and Vismia baccifera subsp. ferruginea, Actual. Biol. 28 (2006) 39–49.

[4] R. Gomez-Cansino, C.I. Espitia-Pinzon, M.G. Campos-Lara, S.L. Guzman-Gutierrez, E. Segura-Salinas, G. Echeverria-Valencia, L. Torras-Claveria, X.M. Cuevas-Figueroa, R. Reyes-Chilpa, Antimycobacterial and HIV-1 reverse transcriptase activity of julianaceae and clusiaceae plant species from Mexico, Evid. Based Complement. Alternat. Med. (2015), 183036.

[5] F. Salas, C. Ciangherotti, M. Salazar-Bookaman, J. Rojas, A. Morales, Toxicidad aguda y actividad analgésica del extracto acuoso de hojas de Vismia baccifera L. var. dealbata (guttiferae) en animales de experimentación, Rev. Fac. Farmac. 49 (2007) 5–9.

[6] T. Utsunomiya, S. Chavali, W. Zhong, R. Forse, Effects of sesamin-supplemented dietary fat emulsions on the ex vivo production of lipopolysaccharide-induced prostanoids and tumor necrosis factor alpha in rats, Am. J. Clin. Nutr. 72 (2000) 804–808.

[7] A.M. Fulton, X. Ma, N. Kundu, Targeting prostaglandin E EP receptors to inhibit metastasis, Cancer Res. 66 (2006) 9794–9797.

[8] A.A. Hussein, B. Bozzi, M. Correa, T.L. Capson, T.A. Kursar, P.D. Coley, P.N. Solis, M.P. Gupta, Bioactive constituents from three vismia species, J. Nat. Prod. 66 (2003) 858–860.

[9] L.J. Lizcano, M. Viloria-Bernal, F. Vicente, L.A. Berrueta, B. Gallo, M. Martinez-Canamero, M.B. Ruiz-Larrea, J.I. Ruiz-Sanz, Lipid oxidation inhibitory effects and phenolic composition of aqueous extracts from medicinal plants of colombian amazonia, Int. J. Mol. Sci. 13 (2012) 5454–5467.


https://doi.org/10.1016/j.heliyon.2018.e00675

[10] L.J. Lizcano, M. Siles, J. Trepiana, M.L. Hernandez, R. Navarro, M.B. Ruiz-Larrea, J.I. Ruiz-Sanz, Piper and vismia species from colombian amazonia differentially affect cell proliferation of hepatocarcinoma cells, Nutrients 7 (2014) 179−195.

[11] J. Trepiana, S. Meijide, R. Navarro, M.L. Hernandez, J.I. Ruiz-Sanz, M.B. Ruiz-Larrea, Influence of oxygen partial pressure on the characteristics of human hepatocarcinoma cells, Redox Biol. 12 (2017) 103−113.

[12] L.J. Lizcano, F. Bakkali, M. Begoña Ruiz-Larrea, J. Ignacio Ruiz-Sanz, Antioxidant activity and polyphenol content of aqueous extracts from colombian amazonian plants with medicinal use, Food Chem. 119 (2010) 1566−1570.

[13] M.M. Bradford, A rapid and sensitive method for the quantitation of microgram quantities of protein utilizing the principle of protein-dye binding, Anal. Biochem. 72 (1976) 248−254.

[14] L. Flohé, W.A. Gunzler, Assays of glutathione peroxidase, Methods Enzymol. 105 (1984) 114−121.

[15] U.K. Laemmli, Cleavage of structural proteins during the assembly of the head of bacteriophage T4, Nature 227 (1970) 680−685.

[16] N. Joza, J.A. Pospisilik, E. Hangen, T. Hanada, N. Modjtahedi, J.M. Penninger, G. Kroemer, AIF: not just an apoptosis-inducing factor, Ann. N. Y. Acad. Sci. 1171 (2009) 2−11.

[17] A. Sancar, L.A. Lindsey-Boltz, K. Unsal-Kacmaz, S. Linn, Molecular mechanisms of mammalian DNA repair and the DNA damage checkpoints, Annu. Rev. Biochem. 73 (2004) 39−85.

[18] I.M. Ward, J. Chen, Histone H2AX is phosphorylated in an ATR-dependent manner in response to replicational stress, J. Biol. Chem. 276 (2001) 47759−47762.

[19] Y. Zhou, Y. Li, T. Zhou, J. Zheng, S. Li, H.B. Li, Dietary natural products for prevention and treatment of liver cancer, Nutrients 8 (2016) 156.

[20] R. Pierini, P.A. Kroon, S. Guyot, K. Ivory, I.T. Johnson, N.J. Belshaw, Procyanidin effects on oesophageal adenocarcinoma cells strongly depend on flavan-3-ol degree of polymerization, Mol. Nutr. Food Res. 52 (2008) 1399−1407.

[21] M.Y. Bonner, J.L. Arbiser, Targeting NADPH oxidases for the treatment of cancer and inflammation, Cell. Mol. Life Sci. 69 (2012) 2435−2442.

[22] S.L. Davies, J. Bozzo, Spotlight on tNOX: a tumor-selective target for cancer therapies, Drug News Perspect. 19 (2006) 223−225.

[23] T. Maraldi, Natural compounds as modulators of NADPH oxidases, Oxid. Med. Cell. Longev. 2013 (2013) 1−10.

 https://doi.org/10.1016/j.heliyon.2018.e00675

[24] D.M. Morre, D.J. Morre, Catechin-vanilloid synergies with potential clinical applications in cancer, Rejuvenation Res. 9 (2006) 45−55.

[25] Y.S. Lee, Role of NADPH oxidase-mediated generation of reactive oxygen species in the mechanism of apoptosis induced by phenolic acids in HepG2 human hepatoma cells, Arch. Pharm. Res. (Seoul) 28 (2005) 1183−1189.

[26] J. Czupryna, A. Tsourkas, Xanthine oxidase-generated hydrogen peroxide is a consequence, not a mediator of cell death, FEBS J. 279 (2012) 844−855.

[27] N. Ballatori, S.M. Krance, S. Notenboom, S. Shi, K. Tieu, C.L. Hammond, Glutathione dysregulation and the etiology and progression of human diseases, Biol. Chem. 390 (2009) 191−214.

[28] F. Wang, S. Liu, Y. Shen, R. Zhuang, J. Xi, H. Fang, X. Pan, J. Sun, Z. Cai, Protective effects of N-acetylcysteine on cisplatin-induced oxidative stress and DNA damage in HepG2 cells, Exp. Ther. Med. 8 (2014) 1939−1945.

[29] E. Santana-Santos, L.H. Gowdak, F.A. Gaiotto, L.B. Puig, L.A. Hajjar, S.P. Zeferino, L.F. Drager, M.H. Shimizu, L.A. Bortolotto, J.J. De Lima, High dose of N-acetylcystein prevents acute kidney injury in chronic kidney disease patients undergoing myocardial revascularization, Ann. Thorac. Surg. 97 (2014) 1617−1623.

[30] P.C. Lin, M.Y. Lee, W.S. Wang, C.C. Yen, T.C. Chao, L.T. Hsiao, M.H. Yang, P.M. Chen, K.P. Lin, T.J. Chiou, N-acetylcysteine has neuroprotective effects against oxaliplatin-based adjuvant chemotherapy in colon cancer patients: preliminary data, Support. Care Cancer 14 (2006) 484−487.

[31] M.A. Khan, H.C. Chen, X.X. Wan, M. Tania, A.H. Xu, F.Z. Chen, D.Z. Zhang, Regulatory effects of resveratrol on antioxidant enzymes: a mechanism of growth inhibition and apoptosis induction in cancer cells, Mol. Cells 35 (2013) 219−225.

[32] T. Kawabe, G2 checkpoint abrogators as anticancer drugs, Mol. Cancer Ther. 3 (2004) 513−519.

[33] M. Baritaud, H. Boujrad, H.K. Lorenzo, S. Krantic, S.A. Susin, Histone H2AX: the missing link in AIF-mediated caspase-independent programmed necrosis, Cell Cycle 9 (2010) 3166−3173.

[34] Z. Zhang, C.Z. Wang, G.J. Du, L.W. Qi, T. Calway, T.C. He, W. Du, C.S. Yuan, Genistein induces G2/M cell cycle arrest and apoptosis via ATM/p53-dependent pathway in human colon cancer cells, Int. J. Oncol. 43 (2013) 289−296.

 https://doi.org/10.1016/j.heliyon.2018.e00675